The Line Shape of Double-Sided Tooth-Disk Waveguide Filters Based on Plasmon-Induced Transparency

2015 Chinese Phys. Lett. 32 054209

(http://iopscience.iop.org/0256-307X/32/5/054209)

CHIN. PHYS. LETT. Vol. 32, No. 5 (2015) 054209

The Line Shape of Double-Sided Tooth-Disk Waveguide Filters Based on Plasmon-Induced Transparency *

ZHANG Xin-Yuan(张新元), WANG Lu-Lu(王鲁橹)**, CHEN Zhao(陈召), CUI Lu-Na(崔鲁娜), SHANG Ce(尚策), ZHAO Yu-Fang(赵玉芳), DUAN Gao-Yan(段高燕), LIU Jian-Bin(刘尖斌), YU Li(于丽)**

School of Science and State Key Laboratory of Information Photonics and Optical Communications, Beijing University of Posts and Telecommunications, Beijing 100876

(Received 2 December 2014)

We numerically investigate a coupled-resonator structure consisting of a stub resonator and a nanodisk resonator using a two-dimensional finite element method. Simulation results show that plasmon-induced transparency (PIT) occurs in the transmission spectra, and the sharp asymmetric Fano lines increase the sensitivity to 1.4×10^3 *nm/RIU. We also analyze the properties of the structure with different radii of the nanodisk and the length of the tooth cavity. Moreover, we find that the PIT only happens when the staggered system is around a fixed location with different separate distances, which is not similar to the previous researches. Our model may be important to photonic-integrated circuits and the sensitivity in sensors.*

PACS: 42.82.Et, 52.25.Fi, 42.82.Gw, 52.35.Hr DOI: 10.1088/0256-307X/32/5/054209

Surface plasmon polaritons (SPPs), which are trapped propagating waves on the surfaces of metal due to the interaction between the free electrons in the metals and photons, can confine and transmit electromagnetic energy in a sub-wavelength limit.[1,2] Surface plasmon polariton waveguides, which utilize the fact that light can be confined at a metal–dielectric interface, are the promising candidates to guide light in nanoscales.[3] The recent activities in exploring plasmonic waveguide structures have been significantly motivated by integration in an optical circuit.[4,5]

By now, a variety of SPP subwavelength optical waveguide devices, such as the bend waveguide device,[6] hybrid plasmonic waveguides,[7] Bragg reflectors,[8] sensors,[9] Y-shaped combiners,[10] Mach–Zehnder interferometers,[11] and nanowires,[12] have been demonstrated experimentally or theoretically. The MIM waveguides consisting of an insulator sandwiched between two metals are a promising structure for design of nanoscale all-optical devices due to strong confinement in the dielectric region with an acceptable propagation length[13,14] and low bend loss.[15] Taking advantage of MIM waveguides, many researchers are committed to the development of functional plasmonic structures, such as U-shaped waveguides,[16] wavelength selective waveguide,[17] filters based on ring resonators,[18] nanodisk resonators,[19] and all-optical switching.[20] Among the SPP-guiding structures mentioned above, optical resonators are crucial structural components in plasmonic wavelength-selective devices owing to their symmetry, simplicity, and ease of fabrication.[21]

In this Letter, double-sided tooth-disk MIM structures are proposed. The transmission spectra of the double-sided structures is discussed as functions of tooth depth and disk radius. In sensing applications, the results show that the sensitivity of the proposed structure is about $S = 1.4 \times 10^3$ nm/RIU and its figure of merit (FOM*) is as high as 4500. This compact plasmonic structure with high sensitivity may be applied as a significant device in on-chip nano-sensors. The transmittance spectrum of a staggered double-sided tooth-disk structure is also addressed.

In the subwavelength MIM structure only the TM mode consisting of E_x, E_z and H_y components is discussed due to its obvious plasmon excitation on the metallic surfaces. The dispersion equation for the TM mode in the waveguide is expressed as[22]

$$\varepsilon_{\rm d} k_{z2} + \varepsilon_{\rm m} k_{z1} \coth\left(-\frac{ik_{z1}}{2} w\right) = 0, \tag{1}$$

where k_{z1} and k_{z2} are $k_{z1}^2 = \varepsilon_{\rm d} k_0^2 - \beta^2$ and $k_{z2}^2 = \varepsilon_{\rm m} k_0^2 - \beta^2$, with $\varepsilon_{\rm d}$ and $\varepsilon_{\rm m}$ defined as dielectric constants of the dielectric medium and the metal, respectively, $k_0 = 2\pi/\lambda_0$ is the wave vector in a vacuum, $n_{\rm eff} = \beta/k_0$ is the effective index of the waveguide for SPPs. In this work, the dielectric is assumed to be air with $\varepsilon_{\rm d} = 1$ and the metal is set as silver. The dielectric constant $\varepsilon_{\rm m}$ of silver is characterized by the Drude model,[23]

$$\varepsilon_{\rm m}(\omega) = \varepsilon_\infty - \frac{\omega_p^2}{\omega(\omega + i\gamma)}, \tag{2}$$

where $\varepsilon_\infty = 3.7$ represents the dielectric constant at infinite angular frequency; $\omega_p = 1.38 \times 10^{16}$ Hz is the bulk plasma frequency, which stands for the natural frequency of the oscillations of free-conduction electrons; $\gamma = 2.73 \times 10^{13}$ Hz is the electron collision frequency, and ω is the angular frequency of the incident electromagnetic wave.

*Supported by the National Natural Science Foundation of China under Grant Nos 11374041 and 11404030, and the Fund of State Key Laboratory of Information Photonics and Optical Communications of Beijing University of Posts and Telecommunications of China.

**Corresponding author. Email: llwang@bupt.edu.cn; bupt.yuli@gmail.com

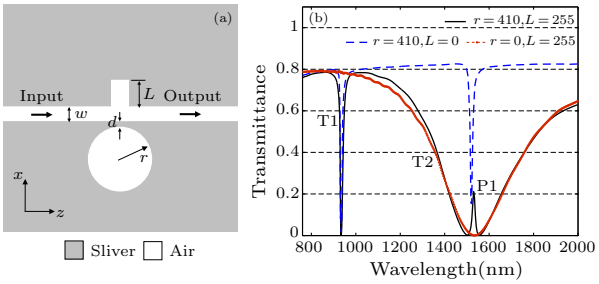

Fig. 1. (a) Schematic diagram of a double-sided tooth-disk nanoplasmonic waveguide. (b) The transmission spectra of a double-sided tooth-disk waveguide filter with $L = 255$ nm, $r = 410$ nm, $d = 10$ nm and of a single-sided tooth-shaped waveguide filter with $L = 255$ nm as well as a disk-shaped waveguide filter with $r = 410$ nm and $d = 10$ nm.

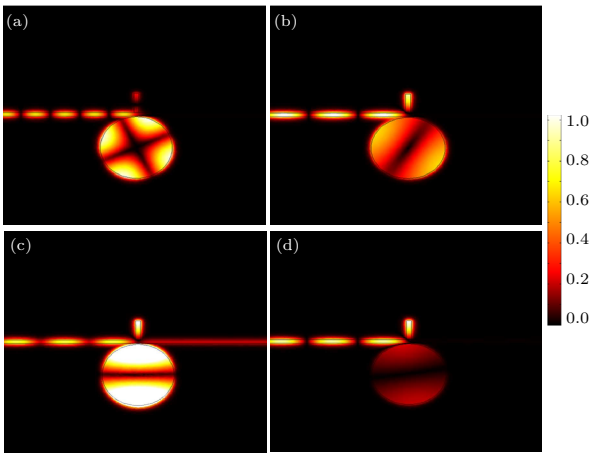

Fig. 2. The $|H_y|$ field distributions at the T1 (a), left dip (b), P1 (c) and right dip (d) in the coupled plasmonic resonator system. The intensity of the field is normalized to units.

Figure 1(a) shows the structure of a proposed double-sided tooth-disk waveguide filter. The waveguide width w is fixed at 50 nm, and L is the depth of the tooth. The distance between the boundaries of the waveguide and the disk cavity is d, and r is the radius of the disk. The fundamental TM mode of the plasmonic waveguide is excited at the left beginning of the waveguide. The transmittance of SPPs is defined as the quotient between the SPP power flows of the output port and input port. The power flows at the ports were obtained by integrating the Poynting vector over the cross section of the waveguide. The transmission spectra of the double-sided tooth-disk waveguide filter (the black solid line) and the single-sided tooth-shaped (the red dotted line) as well as the disk-shaped waveguide filter (the blue dashed line) are shown in Fig. 1(b) for comparison. One can see that there is one trough (T1) at the free-space wavelength of nearly 934 nm with the transmittance of ≈0, which is due to the 2nd-order resonance of the disk resonator in keeping with the $|H_y|$ field distribution shown in Fig. 2(a). There is another trough (T2) at the right of the transmittance spectra. Here T2 is a Lorentzian line shape mainly due to the stub. However at the middle of T2, there exists a peak(P1) of 1530 nm, which is caused by detuned tooth-disk resonators, and this phenomenon is called the plasmon-induced transparency (PIT).[24] Figures 2(b)–2(d) are the field distribution of the left dip, P1 and the right dip in T2, respectively. Near the resonance wavelength of the cavities, the SPPs can be reflected back and forth off the two resonators with high reflectivity, constructing a new resonator in the plasmonic system and resulting in the narrow transmission peak P1. As shown in Fig. 2(d), the SPPs are completely reflected when the stub resonator is nearly at resonance.

To better understand the origin of the PIT, we analyze a single tooth or disk waveguide structure, separately. The middle wavelength λ_m of the trough in the transmission with a single stub is determined as follows:[22,23]

$$\lambda_m = \frac{4n_{\text{eff}}L}{(2m+1) - [\Delta\varphi(\lambda)]/\pi}, \tag{3}$$

where $\Delta\varphi(\lambda)$ is the phase shift brought by reflection on the air–silver surface. It can be seen that the wavelength λ_m is linear to the tooth depth L and depends on the tooth width through the somewhat inverse-proportion relationship with the effective index n_{eff}. Thus when we change the length of L, the left dip and the peak (P1) nearly stay in the same location, while the wavelength of the right dip has a red shift and is linear to the length of the stub in Figs. 3(a) and 3(b), which agrees with the field distribution in Fig. 2(d).

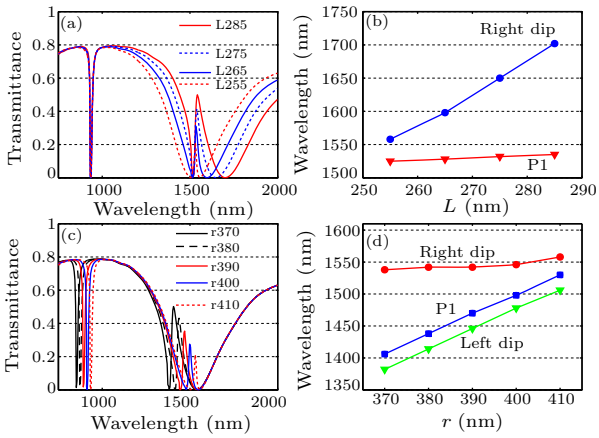

Fig. 3. (a) Transmission spectra of the double-sided tooth-disk waveguide filter for different tooth lengths of L. (b) The wavelengths of the left dip and P1 as a function of L. (c) Transmittance of the double-sided tooth-disk waveguide filter for different radii of the disk cavity. (d) The wavelengths of the left dip, P1 and right dip as a function of r.

When the incident optical wave transmits through a single disk waveguide, part of the energy will couple into the cavity. If the resonance condition is reached, the stable standing modes in the nanodisk segment will be formed. The resonant condition is given by

solving the following equation[19]

$$k_{\rm d}\frac{H_n'^{(1)}(k_{\rm m}r)}{H_n^{(1)}(k_{\rm m}r)} = k_{\rm m}\frac{J_n'(k_{\rm d}r)}{J_n(k_{\rm d}r)}, \tag{4}$$

where $k_{\rm m,d} = k_0 n_{\rm m,d}$ are the wave vectors in the surrounding metal and the dielectric nanodisk, and $n_{\rm m,d}$ are the refractive indices of the metal and the dielectric, respectively, J_n and H_n are the first kind Bessel and Hankel functions with the order n, and J_n' and H_n' are the derivatives of the Bessel and Hankel functions. The first and second resonance modes are discussed in the wavelength range of interest, which correspond to the first and second order of the Bessel and Hankel functions. The trough1 (T1) is the second resonance mode, which can be seen from Fig. 2(a). The peak1 (P1) is related to the first resonance mode, which is shown in Fig. 2(c). From Eq. (4), we can find that the resonance wavelength λ_0 is determined by the refractive index and the radius of the cavity. Figure 3(c) shows the transmission spectrum according to different radii of the nanodisk cavity. It is obvious that T1, left dip and P1 have a blue-shift with decreasing the radius and the symmetric peak (P1) becomes asymmetrically at the same time. This asymmetric peak is the Fano line shape arising from the interference between a localized state due to the coupled resonator system consisting of both stub and nanodisk and a continuum band from the tooth-shape waveguide.[9]

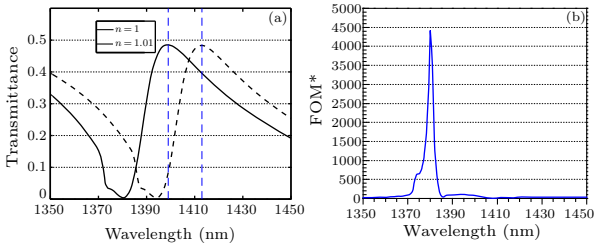

Fig. 4. (a) Transmission spectra of the double-sided tooth-disk waveguide filter for a dielectric area of different refractive indices in sensing applications. (b) Calculated FOM* at different wavelengths.

As shown in Fig. 3(d), the wavelength shifts of the left dip and P1 have a linear relationship with the radius of the nanodisk cavity, which reveal that the location of the left dip and P1 is in accordance with Eq. (4). We also find that the blue line and the green line are paralleled with each other, thus the distance between the central wavelength of the left dip and P1 is constant and the value is 19 nm. As L increases or r decreases more, the distance of the resonate wavelength between the nanodisk and the tooth becomes larger and the strength of coupling becomes weaker. According to the results and the above analysis, one can optimize the Fano line shape by modifying the radius of the nanodisk resonator or the length of the stub.

Due to the sharp asymmetric response line shapes, structures with the Fano resonances exhibit high sensitivity to the index variations of the nearby or surrounding medium, showing great prospects in the applications of nano-plasmonic sensors. According to the Lorentzian-like response line shapes shown by the red lines in Fig. 1(b), from the peak (represented as an 'on' state) to the valley (represented as an 'off' state), the separation of wavelength is about $\Delta\lambda = 350$ nm. This indicates a low sensitivity of response spectra to the index change of the nearby or surrounding medium for the single stub resonator. However it is observed that the transmission spectra (dark solid lines in Fig. 3(c)) in the two coupling resonators become sharp and asymmetric, which is quite different from that in the single-resonator case. For the asymmetric spectra, the transmittance of the SPPs varies sharply from the valley to the peak with only a small wavelength shift of about $\Delta\lambda = 19$ nm, which is considerably smaller than that in the single-resonator case. This reveals that the wavelength shift required for a completely on/off variation is significantly reduced, implying a high sensitivity to the index variations of the nearby or surrounding medium. The pronounced properties in the ultra-small structure, such as the high sensitivity to the index variations as well as the strong field enhancements, can be exploitable in applications of nano-plasmonic sensing.

To prove the validity of the system in the applications, the sensing characteristics of the proposed structure are numerically calculated further, and the results are displayed in Fig. 4. It is observed that the Fano line shapes have a red-shift of about 14 nm when the refractive index of the dielectric area changes from $n = 1.00$ to $n = 1.01$, as shown by the dark line in Fig. 4(a). The sensitivity of a sensor (nm/RIU) is usually defined as the variations in the resonance wavelength per unit change of the refractive index. Thus the sensitivity of the proposed structure is about $S = 1.4 \times 10^3$ nm/RIU.

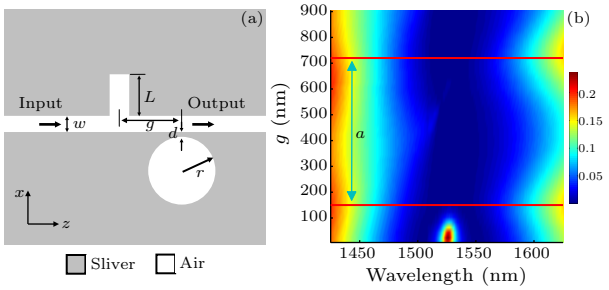

Fig. 5. (a) Schematic diagram of a staggered double-sided tooth-disk nanoplasmonic waveguide with a staggered length of g. (b) Transmission spectra of the double-sided staggered tooth-disk waveguide filter for different staggered lengths with $r = 410$ nm and $L = 255$ nm.

Considering that lasers are vital devices in practice (nearly one-wavelength output), a figure of merit (FOM) at a fixed wavelength can be defined as $\text{FOM}^* = \frac{\Delta T}{T\Delta n}$, where T is the transmittance in the proposed structure. From this equation, we can obtain a large value of FOM* shown in Fig. 4(b) results

from an ultra-low transmittance T and a sharp change $\Delta T/\Delta n$ of the transmittance induced by index variations. It is clear that the FOM* is as high as 4500 at $\lambda = 1380\,\text{nm}$, which is due to the sharp asymmetric Fano line shape with ultra-low transmittance at this wavelength, as shown in Fig. 4(a).

It is also of interest to address a staggered double-sided tooth-disk MIM waveguide structure shown in Fig. 5(a). Here g stands for the staggered length between two single resonators. Figure 5(b) shows how the staggered length of the tooth and the disk influences or modifies the filtering spectrum of the structure. The distance g was adjusted from 5 nm to 905 nm and the corresponding contour plot of the transmission spectra is displayed in Fig. 5(b). It is observed that, firstly, the P1 of the PIT exists only when $g = 0$–$100\,\text{nm}$ and the transmission of P1 reaches the maximum with $g = 25\,\text{nm}$, as shown in Fig. 6(a). It is found that the bandwidth of P1 is about $\Delta\lambda_{\text{FWHM}} = 10\,\text{nm}$, which is much narrower than that of the single stub resonator ($\Delta\lambda_{\text{FWHM}} = 180\,\text{nm}$). Secondly, the width of T2 is periodical as the distance g increases. According to the MIM waveguide dispersion relation Eq. (1), half the effective plasmonic wavelength is $\lambda_{\text{eff}}/2 = 583\,\text{nm}$, which matches the periods obtained by the simulation $a = 580\,\text{nm}$ in Fig. 6(b) well. However, P1 only appears once and the value of P1 is smaller when the disk is at the left of the tooth, which is totally different from that in Ref. [24] and should be further investigated. When $g > 100\,\text{nm}$, the disappearance of P1 in the coupled plasmonic system can induce a broader bandgap compared with that of the individual tooth resonator and can be used as a band-stop filter.

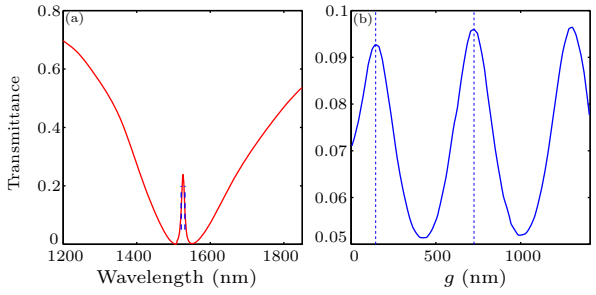

Fig. 6. (a) Transmittance of the double-sided tooth-disk waveguide filter with $g = 25\,\text{nm}$. (b) Dependence of the transmittances on the separation of the two cavities, g, for $\lambda = 1600\,\text{nm}$.

In conclusion, a coupled resonator structure based on a stub resonator and a nanodisk resonator is proposed and calculated by the 2D FEM. When the two cavities are at the condition of detuning, this will lead to PIT and the sharp asymmetric Fano lines will appear due to the difference of the cavities' transmittance. The line shape of the structure may play a great role in filters and sensors. We can obtain the transmission spectra needed by modulating the geometrical parameters. Also a typical filtering function with a wide bandgap will be realized with the sided cavities staggered. In addition, the proposed structures may be applied to highly integrated optical circuits and sensors.

References

[1] Maier S A 2007 *Plasmonics: Fundamentals and Applications* (Berlin: Springer)
[2] Barnes W L, Dereux A and Ebbesen T W 2003 *Nature* **424** 824
[3] Gramotnev D K and Bozhevolnyi S I 2010 *Nat. Photon.* **4** 83
[4] Liu L, Han Z and He S 2005 *Opt. Express* **13** 6645
[5] Xiao S and Mortensens N A 2008 *Opt. Express* **16** 14997
[6] Lee T W and Gray S K 2005 *Opt. Express* **13** 9652
[7] Hu R, Lang P L, Zhao Y F, Duan G Y, Wang L L, Dai J, Chen Z, Yu L and Xiao J H 2014 *Chin. Phys. Lett.* **31** 095202
[8] Gong Y K, Wang L R, Hu X H, Li X H and Liu X M 2009 *Opt. Express* **17** 13727
[9] Lu H, Liu X M, Mao D and Wang G X 2012 *Opt. Lett.* **37** 3780
[10] Gao H, Shi H, Wang C, Du C, Luo X, Deng Q, Lv Y, Lin X and Yao H 2005 *Opt. Express* **13** 10795
[11] Bozhevolnyi S I, Volkov V S, Devaux E, Laluet J Y and Ebbesen T W 2006 *Nature* **440** 508
[12] Ditlbacher H, Hohenau A, Wagner D, Kreibig U, Rogers M, Hofer F, Aussenegg F R and Krenn J R 2005 *Phys. Rev. Lett.* **95** 257403
[13] Mei Z and Zhao D 2004 *J. Opt. Soc. Am.* A **21** 2375
[14] Veronis G and Fan S 2005 *Appl. Phys. Lett.* **87** 131102
[15] Neutens P, Dorpe P V, Vlaminck I D, Lagae L and Borghs G 2009 *Nat. Photon.* **3** 283
[16] Lee T and Gray S 2005 *Opt. Express* **13** 9652
[17] Wen K, Yan L, Pan W, Luo B, Guo Z and Guo Y 2012 *J. Opt.* **14** 075001
[18] Wang T B, Wen X W, Yin C P and Wang H Z 2009 *Opt. Express* **17** 24096
[19] Zhan G Z, Liang R S, Luo J and Zhao R T 2014 *Opt. Express* **22** 9912
[20] Lu H, Liu X, Mao D, Gong Y and Wang G 2011 *Opt. Lett.* **36** 3233
[21] Chremmos I 2009 *J. Opt. Soc. Am.* A **26** 2623
[22] Chen Z, Song G and Yu L 2012 *Chin. Phys. Lett.* **29** 104210
[23] Chen Z, Yu L and Wang L L 2013 *Chin. Phys. Lett.* **30** 054212
[24] Yun B F, Hu G H and Cui Y P 2013 *Opt. Commun.* **305** 17